SANDIA REPORT

SAND2000–8245
Unlimited Release
Printed June 2000

The Effect of Thermal Aging on The Mechanical Properties of a Stockpile Polyurethane Foam

S. H. Goods, L. L. Whinnery

Prepared by
Sandia National Laboratories
Albuquerque, New Mexico 87185 and Livermore, California 94550

Sandia is a multiprogram laboratory operated by Sandia Corporation, a Lockheed Martin Company, for the United States Department of Energy under Contract DE-AC04-94AL85000.

Sandia National Laboratories

Issued by Sandia National Laboratories, operated for the United States Department of Energy by Sandia Corporation.

Available to DOE and DOE contractors from
Office of Scientific and Technical Information
P.O. Box 62
Oak Ridge, TN 37831

Prices available from (703) 605-6000
Web site: http://www.ntis.gov/ordering.htm

Available to the public from
National Technical Information Service
U.S. Department of Commerce
5285 Port Royal Rd
Springfield, VA 22161

NTIS price codes
Printed copy: A03
Microfiche copy: A01

SAND2000-8245
Unlimited Release
Printed June 2000

THE EFFECT OF THERMAL AGING ON THE MECHANICAL PROPERTIES OF A STOCKPILE POLYURETHANE FOAM

S. H. Goods
Materials Mechanics Department

L. L. Whinnery
Materials Chemistry Department
Sandia National Laboratories
Livermore, California 94551-0969

ABSTRACT

The influence of thermal aging on the uniaxial mechanical properties of BKC44402, a stockpile polyurethane foam is examined. High rate impact tests revealed a marked decrease in energy absorption for specimens aged at 60°C and 80°C after only 7 months of aging. At one year, even specimens aged at ambient room temperature conditions have shown signs of decreased energy absorption. This loss in toughness results from the onset of brittle fracture at relatively small compressive strains. Further, spallation of material is observed as the foam is compressed during impact. In contrast, conventional, quasi-static tension and compression behavior is unaffected through 1 year of aging at temperatures up to 80°C. Neither fracture nor spallation was observed in these latter tests.

TABLE OF CONTENTS

FIGURES

THE EFFECT OF THERMAL AGING ON THE MECHANICAL PROPERTIES OF A STOCKPILE POLYURETHANE FOAM

I. Introduction

TDI-based polyurethane foams are found in every weapons system in the stockpile. The most common of these foams is designated BKC44402 and has been used routinely for over 25 years. These foams are used for a variety of reasons; they may be used simply as volume fillers or to afford electrical isolation. In other applications, however, they may be required to mitigate vibration or impact. As such, changes in the mechanical properties of these foams as they age in the stockpile may affect their performance. Notwithstanding this, there is little documented information describing time and temperature induced changes in the mechanical and physical properties of these foams.

Some accelerated aging studies have shown that these polyurethane foams can suffer changes in their viscoelastic characteristics as the result of laboratory aging. For example, Rand and Ulibarri [1] have reported changes in the loss and storage moduli as well as shifts in the glass transition temperature (Tg) for polyurethane foams as determined by DMA (Dynamic Mechanical Analysis) measurements. Figure 1a and b shows that the loss and storage moduli for BKC44402 increase by 20% and 30% respectively after elevated temperature aging for two years. Figure 1c reveals that the Tg for another polyurethane foam, BKC44307, decreased by about 7% after 2 years of aging at 80°C. However, it is unclear if there exists any relationship between these dynamic property measurements and the more conventional kinds of physical and mechanical properties (Young's modulus, collapse strength, toughness etc.) that a designer might use in specifying a particular foam or set of performance requirements.

This study was undertaken in order to directly assess the effect of thermal aging on conventional mechanical properties of a stockpile foam as part of the Enhanced Surveillance Program. Three different types of testing were identified as relevant to stockpile environments: high rate impact tests for the determination of energy absorption characteristics and crush strength, and quasistatic compression and tension testing for the determination of modulus, collapse strength (compression) and fracture stress/strain (tension). Our intention was to then correlate any measured changes with DMA measurements similar to those reported in Reference 1. This report summarizes initial findings with respect to mechanical behavior through one year of aging of representative stockpile foam.

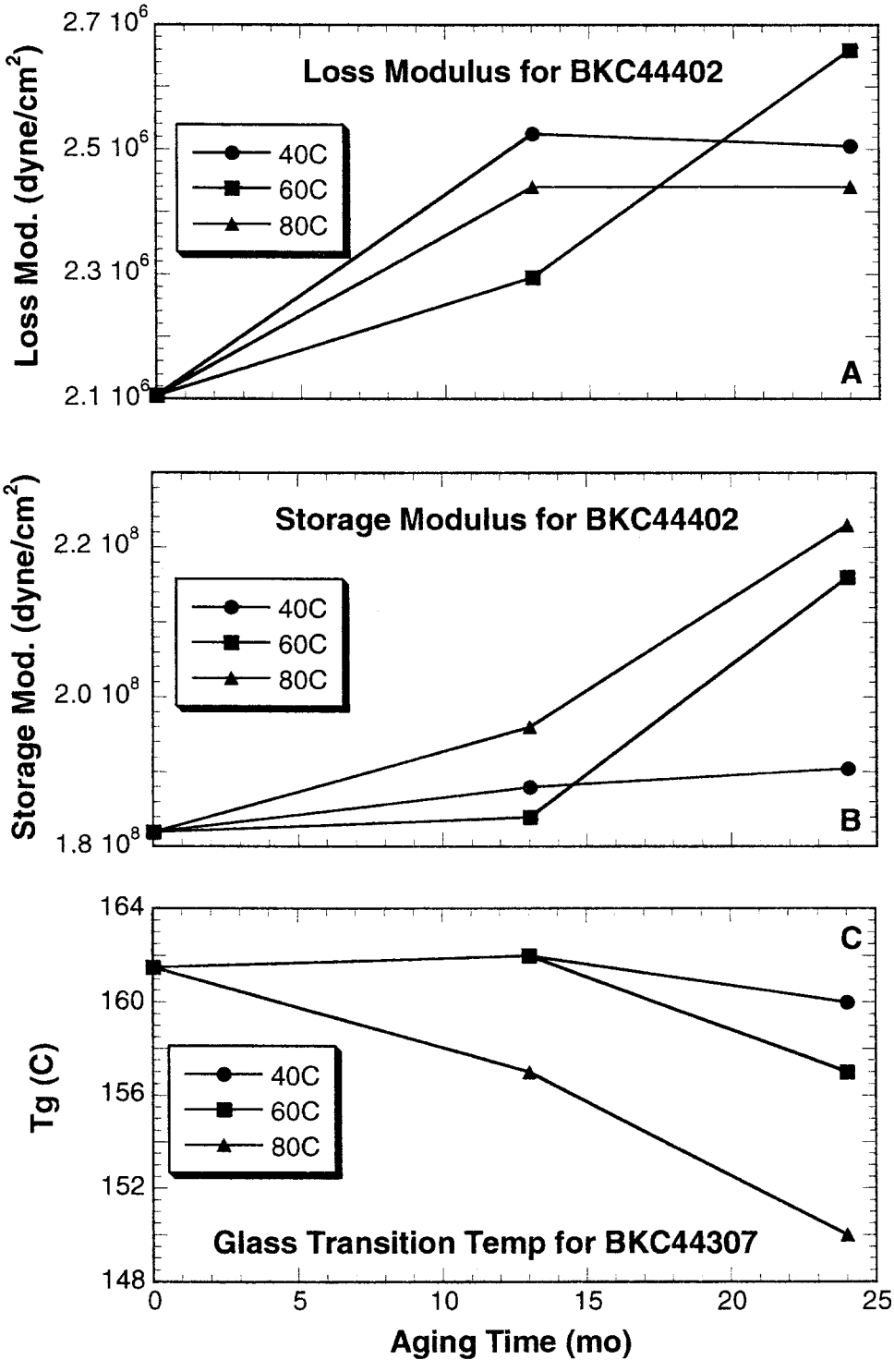

Figure 1. Thermal aging effects on polyurethane foam on DMA derived properties Reference 1.

II. Experimental Procedures

Material

The foam chosen for this study was BKC44402. As stated previously, this TDI-based polyurethane foam is the one that is the most ubiquitous in the stockpile. The target density for the foam specimens was 0.1 g/cm^3 ($\approx$ 6 lb/ft^3) which is within the range of densities that it finds use. The foam for this study was produced at SNL/CA from kits obtained from Honeywell Federal Manufacturing and Technologies, in Kansas City. The BKC44402 kit consists of an "R component" and a "T component". Each of these components is comprised of the following constituents:

TABLE 1. CONSTITUENTS OF BKC44402 KIT

R component			
Ingredient	Parts per hundred	Function	Supplier
R513	87.5	Polyol	Stepan
R514	12.5	Polyol	Stepan
DI water	1.79	Blowing agent	
L5320	1.5	Surfactant	OSI Witco
T Component			
TDI Prepolymer	168.5	Isocyanate	Honeywell FMT

The T component is actually a mixture of TDI (65%) and an isocyanate terminated copolymer (35%) of adipic acid, TDI trimethylolpropane, phthalic anhydride and diethylene glycol.

Processing

In a typical batch, 1537 g of the R component and 3280 g of the T component were weighed into an 8 L plastic container. The combination was mixed with a 10.2 cm (4 inch) diameter Conn blade in a drill press (approximately 1800 rpm) for 1 minute. The sides and bottom of the mixing container were continuously scraped by the Conn blade during mixing to help ensure adequate incorporation of the viscous R component from the container surface. The contents were then poured into a 20 L plastic container and allowed to rise and gel under ambient conditions. After at least 2 hours at room temperature, the billet was heated at 65°C for 4 hours.

Aging

Blocks of foam were then cut into cubes that measured 6.4 cm on a side and their masses were recorded. These blocks were then placed in ovens to age for predetermined periods of time from one week to four years. The actual aging time intervals for this study are: 1 week, 3 months, 7 months, 1 year, 2, years, 3 years and 4 years. At this writing, testing has been completed on specimens up to and including 1 year of aging. Two elevated temperatures were chosen, 60°C and 80°C. The higher of these temperatures is somewhat above the nominal maximum STS temperature that is typically quoted for weapon systems (71°C), but allowed us to compare our results with other relevant work. An additional set of blocks was set aside to age at the nominal laboratory ambient temperature for the same time intervals. After each aging interval the cubes were re-

weighed to determine mass changes and then specimens machined to final dimensions. By machining the actual test specimens from the core of each of these blocks, the effect of near-surface oxidation was minimized.

Test Specimens/Mechanical Testing

At the end of each aging interval, foam blocks aged at each of the three temperatures were selected for testing and machined to final dimensions. Two specimen geometries were used. For impact and quasi-static compression testing right circular cylinders were used. These specimens measured 40 mm in diameter and 51 mm in length. Tensile specimens were somewhat more complex. These specimens were right cylinders (28.7 mm in diameter and 51 mm in length) that were bonded to pull stubs using Hysol EA 3909.NA adhesive. A gage section (19 mm diameter x 25.4 mm length) was then machined into each cylinder. Both specimens are shown in Figure 2.

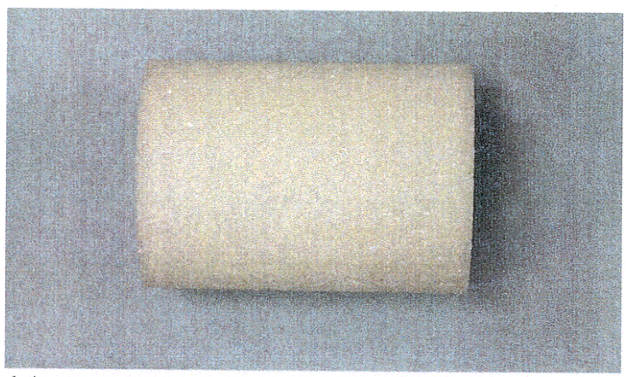

(a)

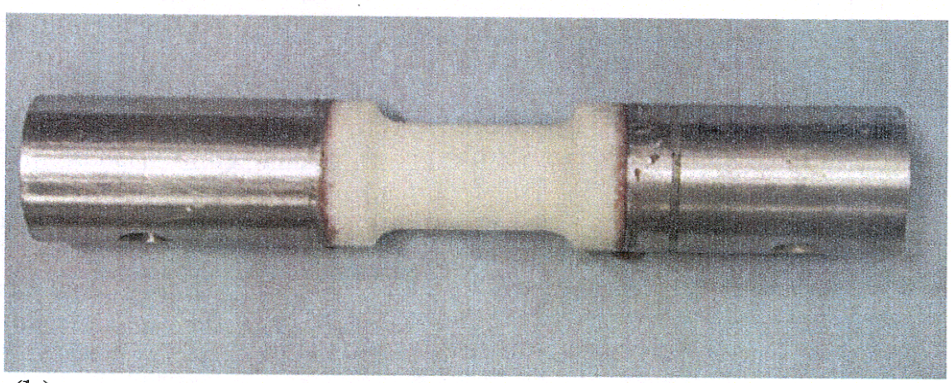

(b)

Figure 2. Specimen geometries used in this study. (a) Impact and compression specimens were right cylinders 40 mm in diameter and 51 mm in length.(b) Tensile specimens were bonded to pull stubs. A gage section (19 mm diameter x 25.4 mm length) was then machined into each cylinder.

At each aging interval, twelve samples were removed for each aging temperature. Three were machined into samples for tensile testing and nine for compression and impact.

Typically, three of each test was performed and the data shown represent the average results of those tests.

Energy absorption (toughness) and crush strength under impact conditions were characterized as a function of aging temperature and time. Impact tests were performed on a Dynatup Model 8250 drop weight impact tester coupled to a digital data acquisition and analysis system. The drop hammer and frame were configured to generate an incident initial strain rate of $\approx 50\ sec^{-1}$. Mechanical stops are necessary to protect the load and displacement transducers from overload or physical damage and were set to limit total compressive engineering strain to ≈ 0.6. Two channels of data were recorded for these tests: load from an instrumented tup (load cell) and displacement from a high-speed, differential variable reluctance transducer (DVRT). These data could then be processed to generate stress-strain curves. All tests were conducted at ambient room temperature.

Modulus, collapse strength and fracture behavior were assessed through a series of quasi-static compression and tension tests performed on a Satec EMP22 mechanical test frame. Load was measured using a 225 kg(f) Interface load cell and an Electronic Instrument Research non-contacting laser extensometer was used to measure displacement. All tests, directed at assessing aging effects, were conducted at ambient room temperature and at an initial strain rate of $2.5 \times 10^{-3}\ sec^{-1}$. Some additional tests were conducted on unaged specimens for the purpose of establishing baseline behavior. Specifically, the influence of strain rate was examined through a series of compression tests performed at rates between. $2 \times 10^{-6}\ sec^{-1}$ and $1 \times 10^{2}\ sec^{-1}$. Lastly, the effect of test temperature was examined through a series of tests conducted at temperatures between -50°C and 80°C (at a single strain rate of $2.5 \times 10^{-3}\ sec^{-1}$).

III. Results

Mass Change

Aging induced changes in the mass were tracked as a function of time and temperature. Figure 3 shows the change in mass for specimens aged up to one year at each of the three temperatures. For specimens aged at room temperature, there is an initial increase in mass due, most likely, to adsorption of moisture from the ambient laboratory environment. With further aging this increase plateaus and may show signs of reversing at the longest aging interval. Specimens aged at 60°C and 80°C exhibit the opposite behavior. In both instances, there are abrupt mass losses due to desorption of moisture in the aging ovens. After the initial sampling interval, there is a gradual and sustained decrease in mass, possibly due to loss of the surfactant used during the formulation of the foam. Preliminary observations from another study have suggested that surfactant migration to free surfaces can occur over time in similar foam systems. (2)

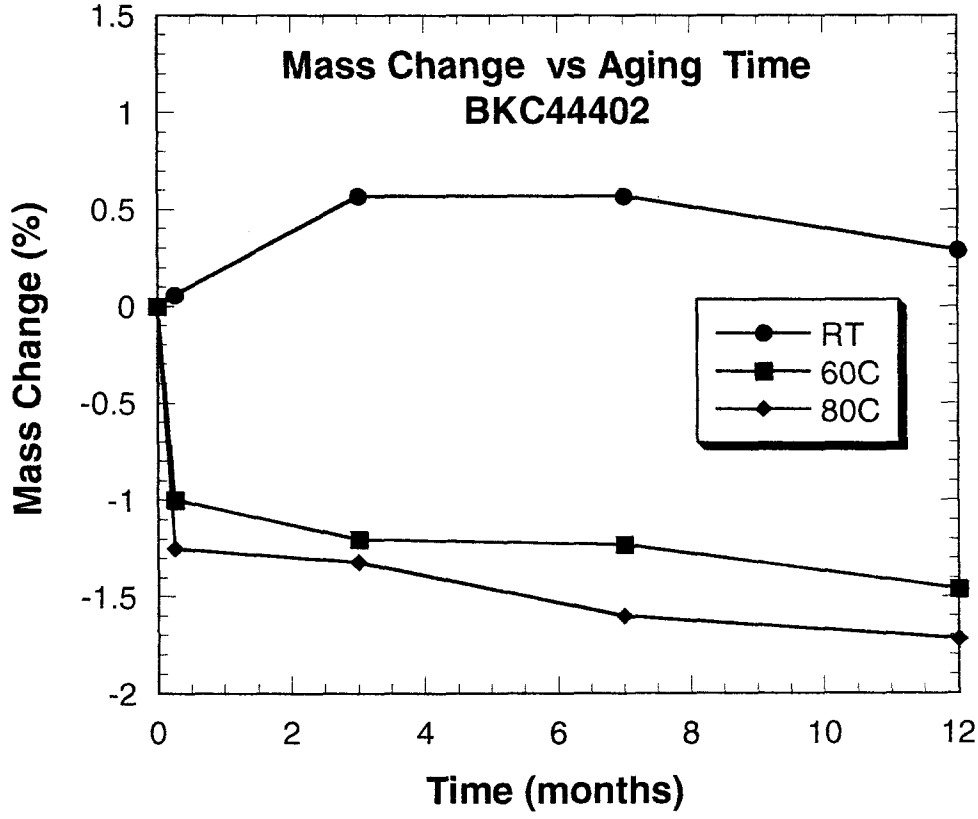

Figure 3. Weight change as a function of time for BKC44402.

Baseline Compression Behavior

Baseline quasi-static mechanical properties of BKC44402 in compression were determined as a function of both strain rate (at ambient temperature) and as a function of temperature (at one nominal strain rate). Figure 4 shows the stress-stain behavior for a

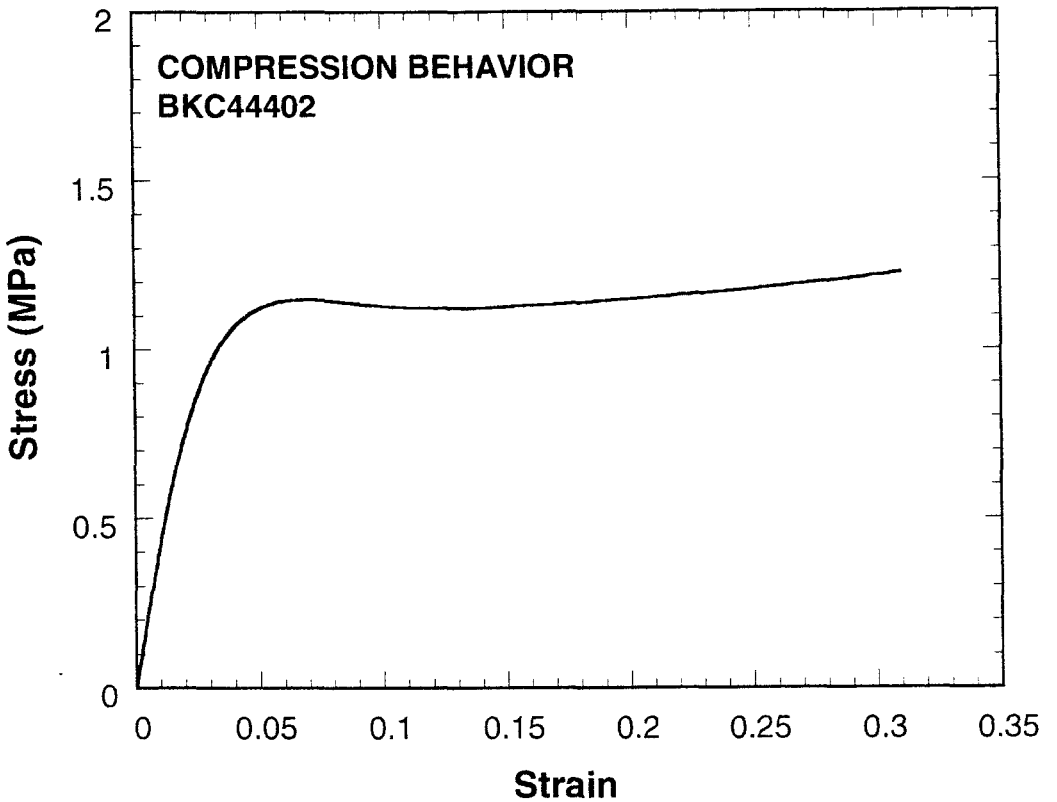

Figure 4. Typical compression curve for BKC44402. Initial linear loading is followed by an abrupt transition to a plateau regime during which the stress remains nearly constant as strain increases.

Specimen ($\rho \approx 0.1$ g/cm^3) tested in compression at an initial strain rate of 2.5×10^{-3} sec^{-1}. As is typical for polymer foams, the specimen loads rapidly at small strains. The slope of this initial linear loading defines the modulus of the foam. There is then an abrupt transition to a plateau region where the stress is nearly constant with increasing strain. This plateau stress is referred to as the collapse or compressive strength of the foam. There is often a yield point at the onset of the plateau region. This yield point can be more pronounced at high strain rates or low foam densities. At larger compressive strains, the stress will begin to rise as the free volume of the foam structure decreases. Over the course of these low strain rate tests, specimens remain intact. There is no tendency for the foam to either crack or spall even at very large strains in excess of 0.6.

Because the foam is comprised of a polymer material, it is inherently viscoelastic. As such, its mechanical properties will depend on both the imposed strain rate, as well as test temperature. In order to establish the rate sensitivity, a series of tests were performed over a wide range of strain rates. Figures 5a and 5b show the rate dependence of the modulus and collapse strength respectively. It is clear from the figure that both the modulus and strength exhibit power law dependencies with respect to the imposed strain rate. While the collapse strength of the foam is more rate sensitive than

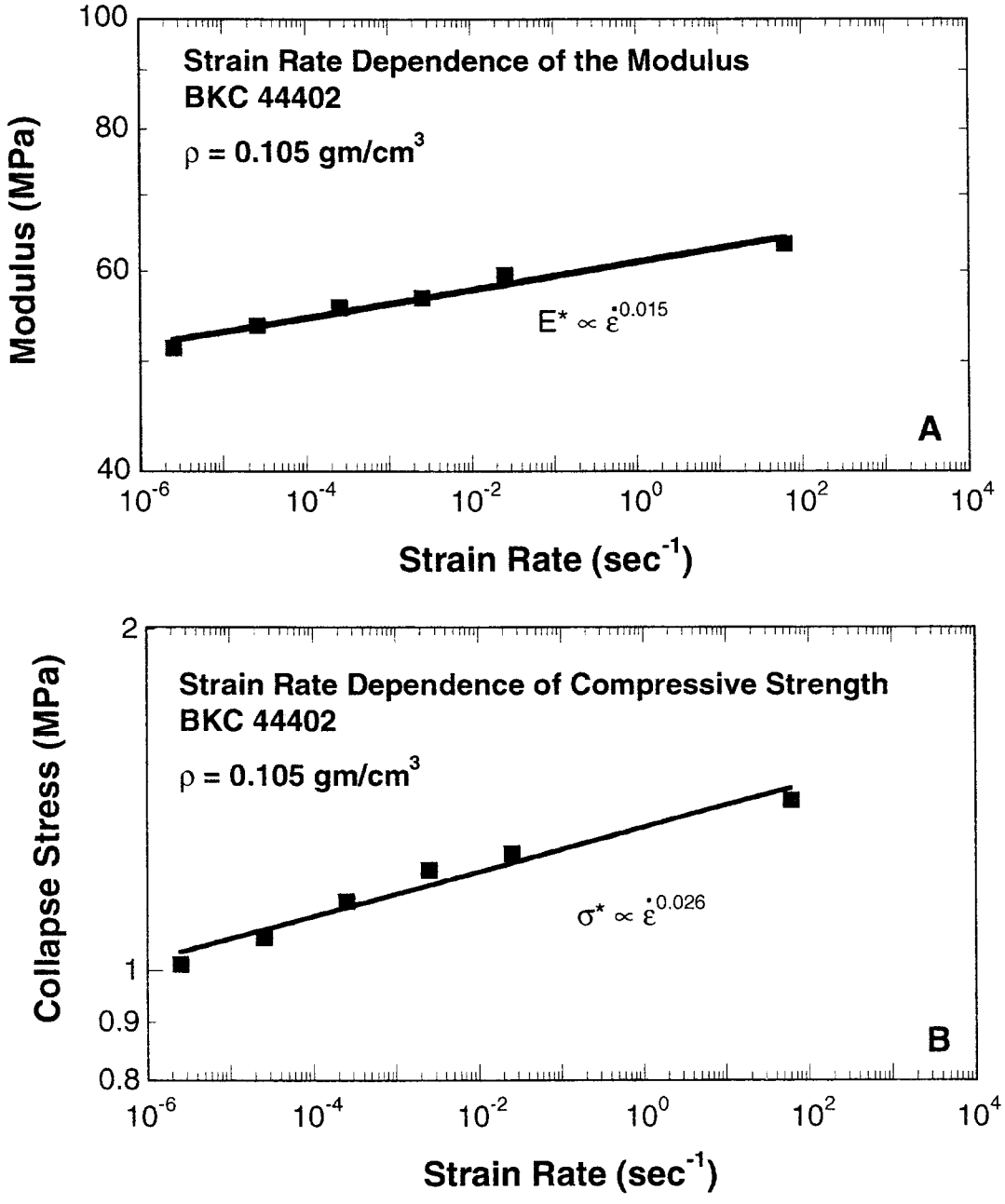

Figure 5. (a) Strain rate dependence of the modulus and (b) collapse stress. Both exhibit a power law dependence with respect to strain rate.

the modulus, neither material parameter is very sensitive to strain rate. Test temperature has a more significant influence on compression properties. Figures 6a and 6b show the effect of test temperature on modulus and strength for tests performed between –50°C and +80°C, well below the glass transition temperature (Tg). In this Figure, the lower abscissa shows the test temperature T normalized by the glass transition temperature (Tg = 135°C) of the polymer while the upper abscissa is the actual test temperature. The

Figure reveals that the strength of the foam doubles over the range of test temperature while the modulus increases by only about 30% between the temperature extremes.

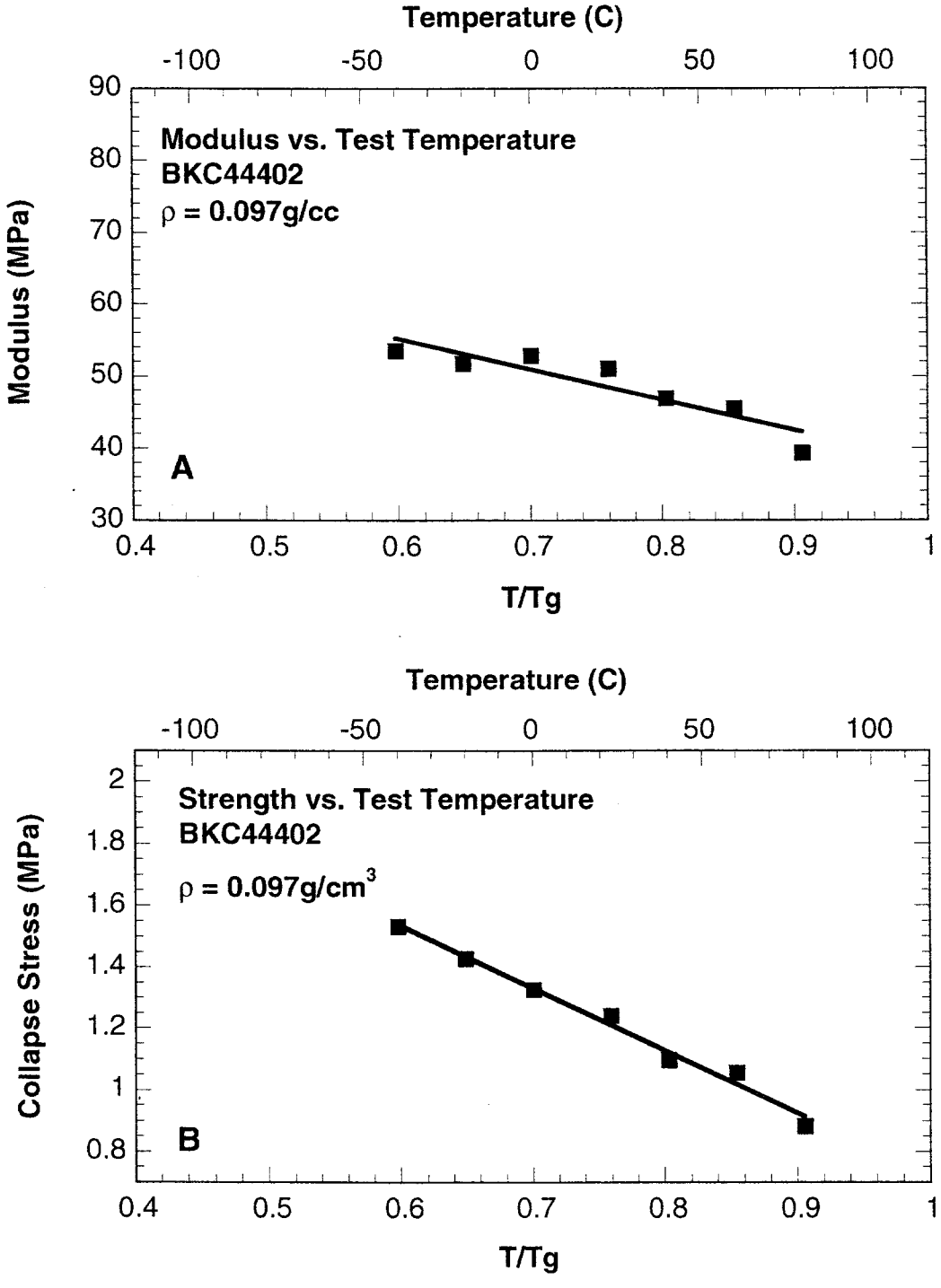

Figure 6. Temperature dependence of the (a) modulus and (b) collapse stress.

Aging Effects

impact behavior-

Two parameters were tracked as indicators of thermal aging effects under impact loading conditions. The first of these, energy absorption, is calculated as the area traced out by the impact stress-strain curve and has the unit energy/volume. The second is the collapse or crush strength and is equivalent to the yield point stress described above for conventional compression testing. Figure 7 shows three impact traces for unaged foam specimens (that is, specimens machined and tested within a few days of the casting of the foam billet). The Figure indicates that, generally, the impact behavior of the three specimens is reproducible. The average collapse or crush strength of the specimens shown in this figure is ≈ 1.38 MPa while the average energy absorption is ≈ 0.72 J/cm^3. The most important feature to note in this figure is that after the collapse stress is reached, the stress remains constant or rises slightly. This indicates that the specimens remain intact over the entire range of compression Note that as indicated in an earlier section, strain is limited to ≈ 0.6. The unloading slope shown in Figure 7 and in later figures indicates that there was some rebound of the specimen after the maximum strain was reached.

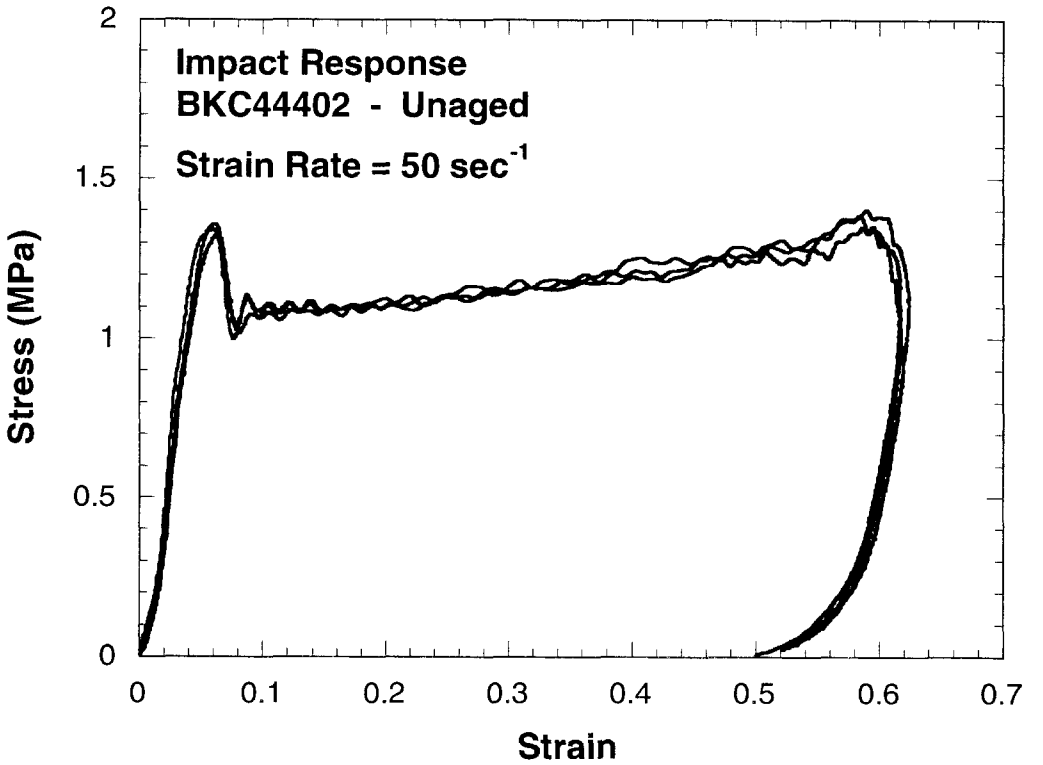

Figure 7. Baseline impact curves for BKC44402. Area traced by the stress-strain curves is defined as the energy absorption and has units of J/cm^3.

Figures 8a and 8b show the impact response of foam specimens after 7 and 12 months of aging at each of the three temperatures. In Figure 8a, the specimen aged at room temperature behaves identically to the unaged specimens shown in the previous figure.

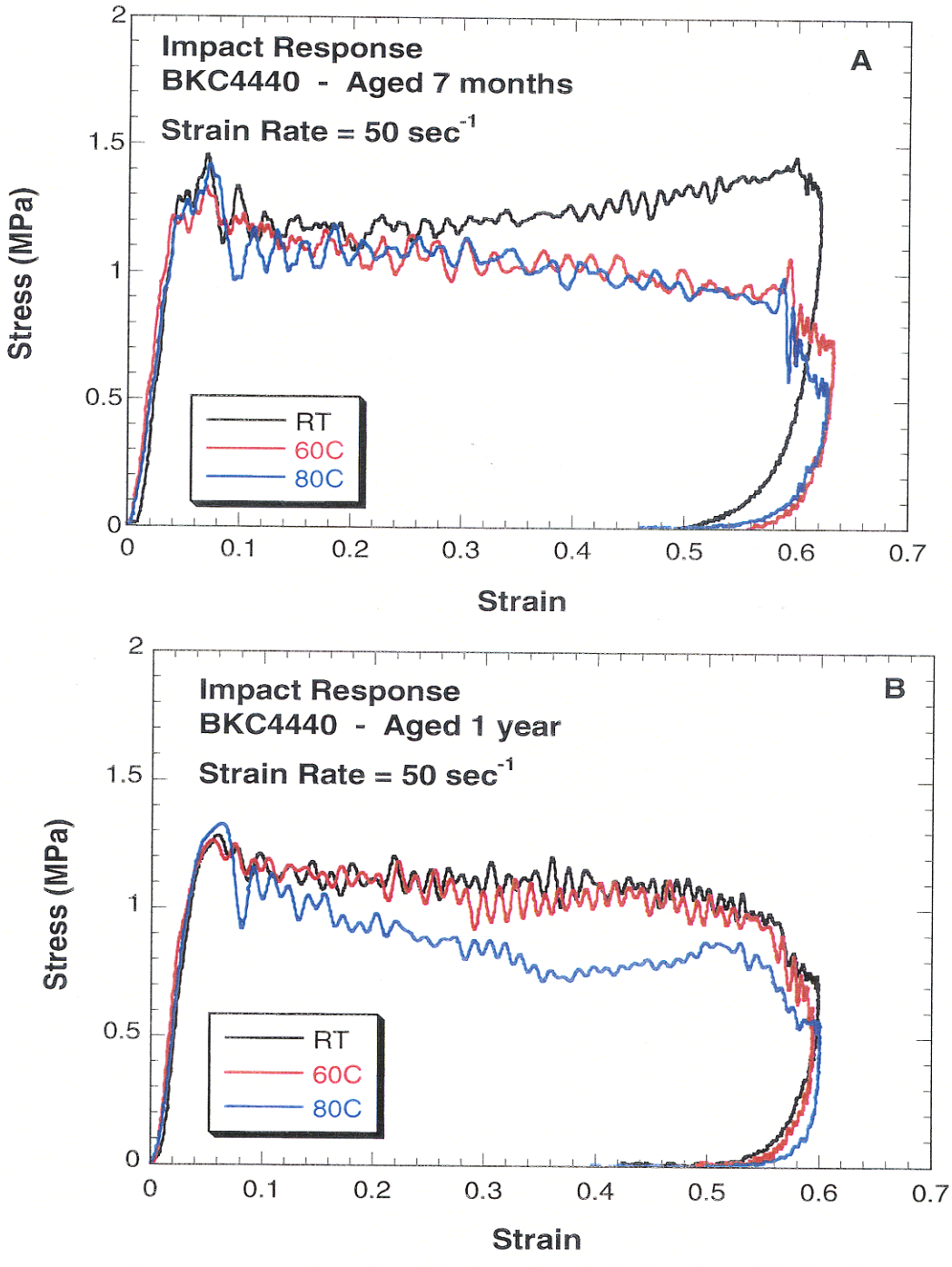

Figure 8. (a) Impact curves after seven months of aging. (b) Impact traces after one year of aging

That is, once the crush strength of the foam is reached, there is the typical sustained stress plateau. As the strain level increases the stress gradually rises as the free volume of the specimen is reduced. However, the specimens aged at the two elevated temperatures exhibit somewhat different behavior. In these instances, once the crush strength is reached, there follows a gradual decrease in stress. This results from the fracture and spalling of the specimens after they begin to crush down. As the specimens fracture and spall, foam is ejected from beneath the striker and the constant stress cannot be sustained, as is the case for the unaged specimens. As a result the energy absorption capabilities of the aged foam specimens is reduced. Figure 8b shows similar impact traces for specimens aged for 1 year. In this instance, all of the specimens, including the specimen held at room temperature, display this characteristic load shedding after the onset of collapse.

Figures 9a and 9b graphically show the very different response to impact of two specimens aged for 7 months. In Figure 9a, a specimen aged at room temperature is shown on the test stage of the drop tower immediately after testing. The specimen is intact and has only compressed axially. In contrast, Figure 9b shows the response of a specimen aged at 80°C for the same period of time. In this figure there is massive spalling of foam from the specimen surface and the ejection of foam debris all around the test stage.

Figures 10 and 11 clearly illustrate the fracture and spalling response of all of the aged specimens tested after 7 months and 1 year of aging. Figure 10 shows all of the specimens tested under impact conditions after 7 months of aging. It is clear that those aged at room temperature (the specimens in the first row) are intact and have simply been compressed axially during impact. In contrast, those aged at elevated temperatures show clear evidence of spalling and fracture. Further, those aged at 80°C show demonstrably greater damage than those aged at 60°C. Figure 11 shows a similar array for specimens aged 1 year. In this instance, even the specimens aged at ambient temperature show clear evidence of spalling.

Figures 12a and 12b summarizes the effect of thermal aging on impact properties of BKC44402. Figure 12a shows the energy absorption charateristics of the. Each column represents the average of three replicate tests performed for each of the aging conditions and the numerical values are indicated at the top of each column. The data are grouped by aging temperature and for each group, the aging period is indicated by the white text label within each column. The horizontal line represents the baseline average energy absorption. Comparing the baseline energy absorption values to those for the aged specimens, it is evident that there has been between a 12% (at 60°C) and 22% (at 80°C) loss in toughness for the specimens aged for the longest time interval. Figure 12b is a similar plot that summarizes the changes in crush strength of the foam under impact conditions. The figure indicates that there has been only a slight reduction in the strength of the foam, even at the longest time interval and at the highest temperatures. Testing at longer time intervals will confirm whether or not there is a trend in this regard.

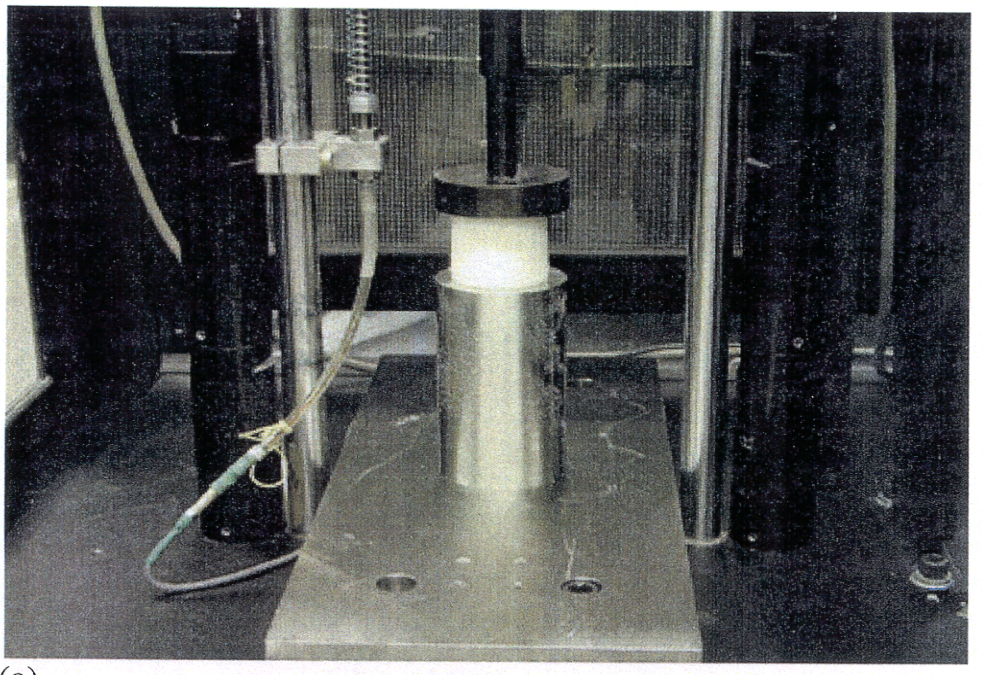

(a)

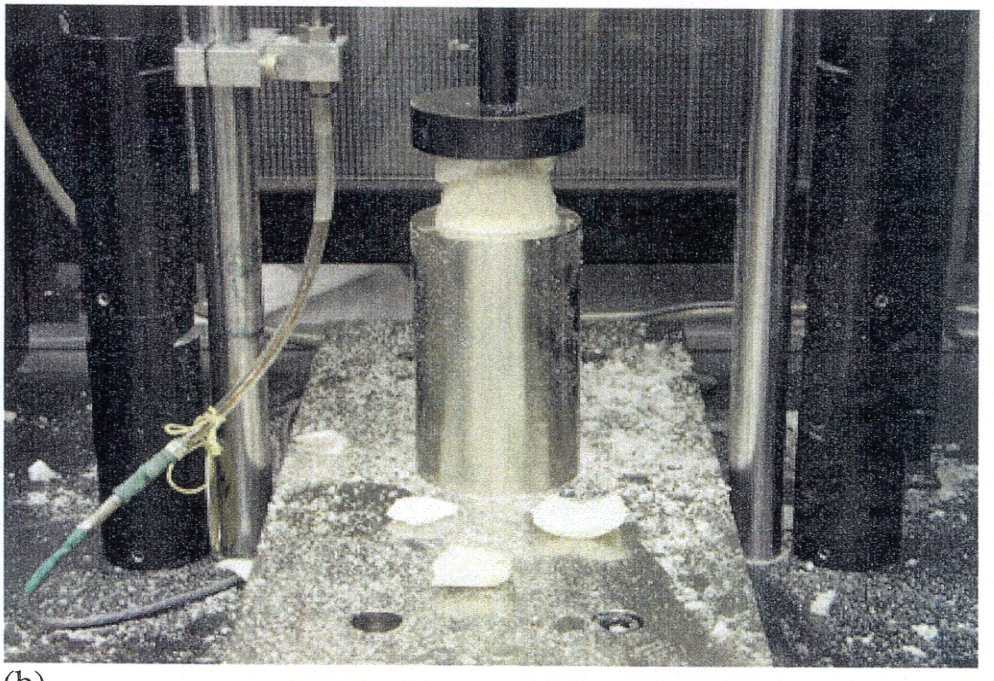

(b)

Figure 9. (a) Specimen aged at room temperature for 7 months is intact. (b) Specimen aged at 80°C for 7 months exhibits spalling and ejection of polymer debris.

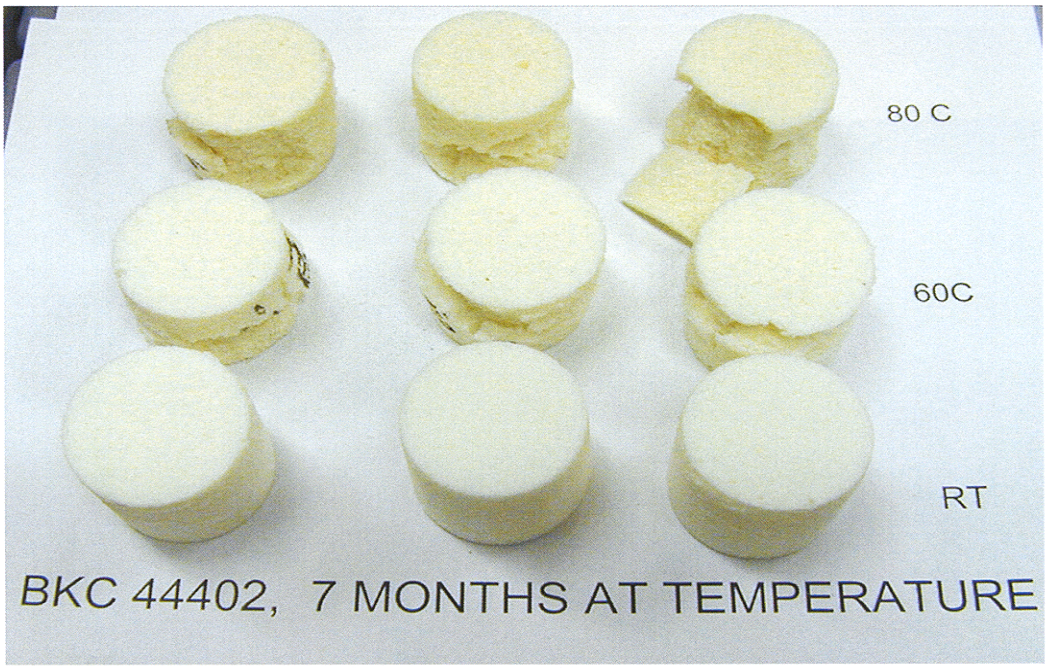

Figure 10. Specimens aged at 60°C and 80°C crack and spall in response to impact testing. Specimens aged at room temperature remain intact.

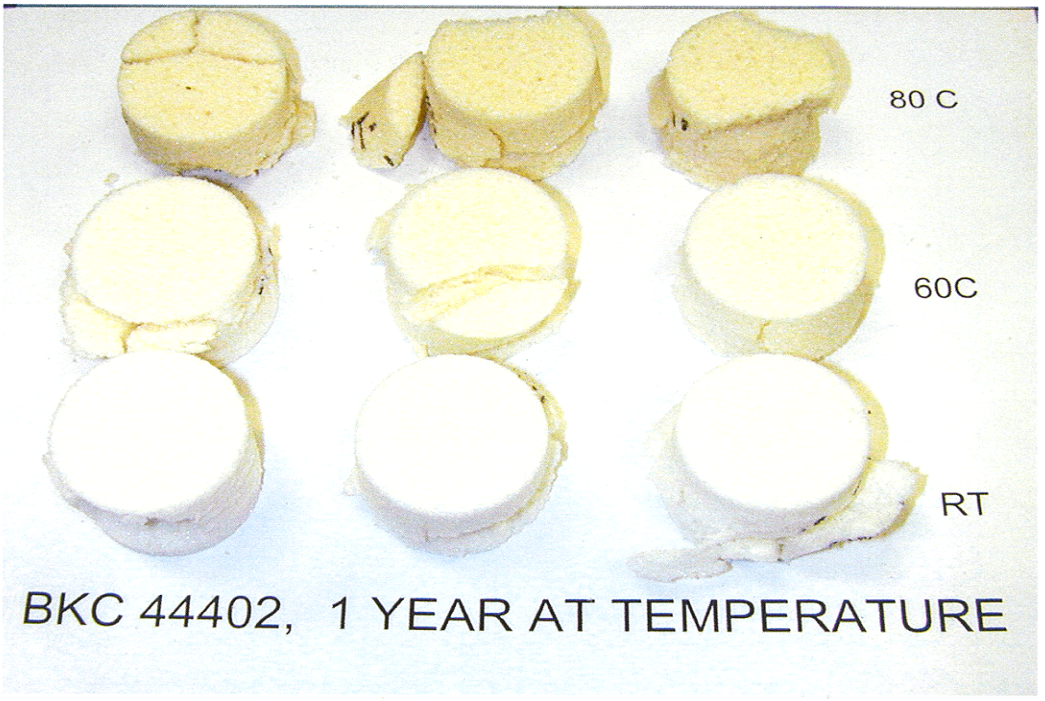

Figure 11. After one year of aging all specimens exhibit damage after impact testing.

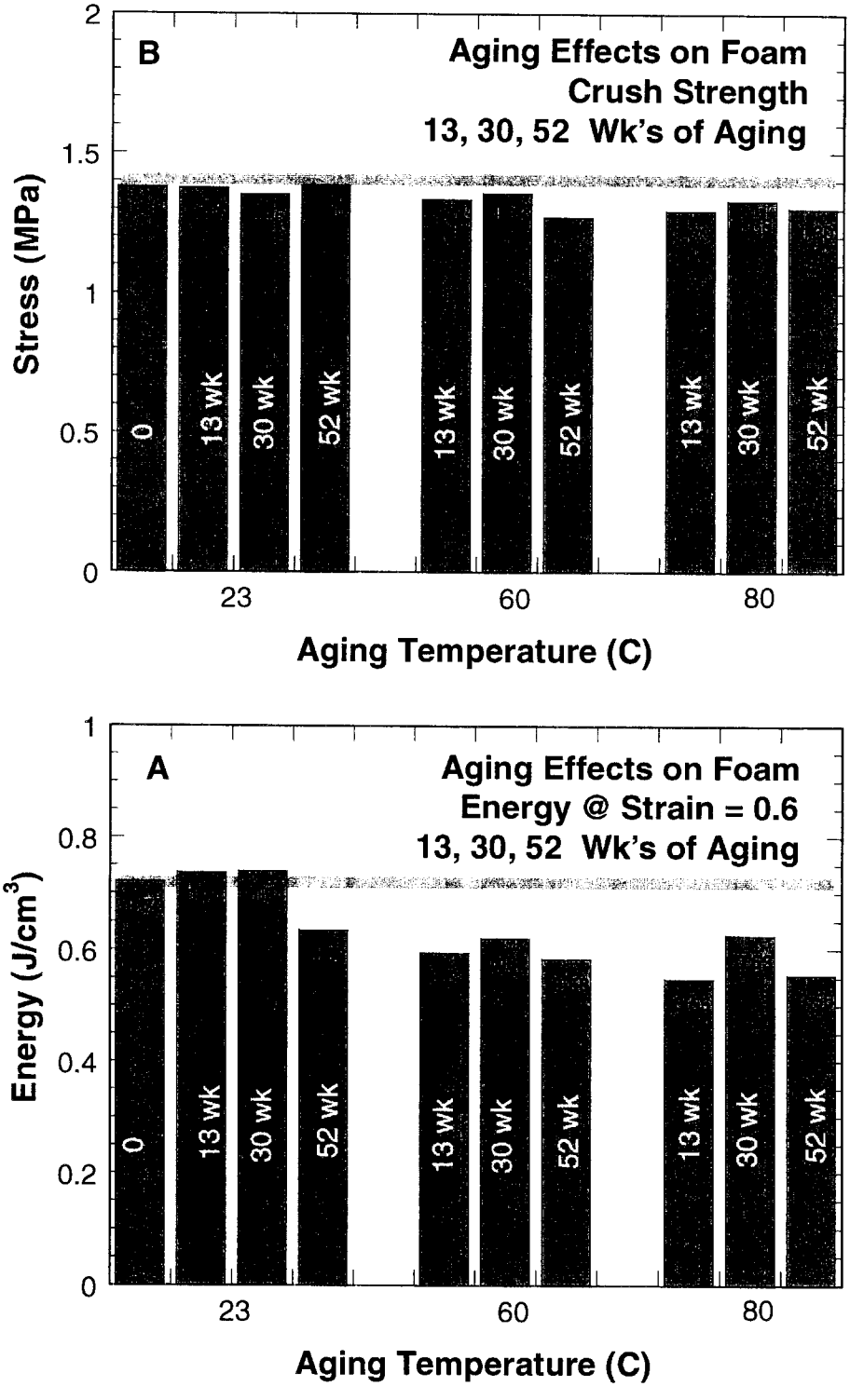

Figure 12. Summary of aging data for impact testing. (a) Modulus shows progressive decrease with increasing aging time and temperature. (b) Crush strength shows little change as the result of aging.

compression behavior-

Unlike the impact specimens, there was no tendency for the specimens tested under quasi-static compression to fracture or spall with increasing aging temperature and time. Changes due to aging, if any, were therefore expected to be more subtle. Because of this, the influence of the small sample-to-sample variations in density were thought to be important. While the target density of the foam specimens was 0.1 g/cm^3, it was not uncommon for individual specimens to vary by ± 3-5%. Previous work [3-5] have shown that both modulus and strength vary with power-law dependencies on density. In the former case, the measured modulus, E_m, is related to density as:

$$E_m \propto E_s \left(\rho / \rho_s \right)^{1.7} \tag{1}$$

where E_s and ρ_s are the modulus and density of the solid polymer and ρ is the density of the foam specimen. In the latter case, collapse strength has been shown to vary with density as:

$$\sigma_m \propto E_s \left(\rho / \rho_s \right)^{2.1} \tag{2}$$

where σ_m is the measured collapse strength of the foam and all other terms are as before. Because of the exponential dependence of E_m and σ_m on density, small variations in ρ are magnified in terms of the scatter in modulus and strength. For example, a 5% density variation can result in more than a 10% variation in strength even in the absence of an aging effect. To account for small density variations between specimens, modulus and strength values derived from the compression tests have been normalized to the nominal target density of 0.1 g/cm^3. Specifically, moduli derived from the slope of the compression curves are corrected as:

$$E = E_m \left(0.1 / \rho \right)^{1.7} \tag{3}$$

where E is the reported density corrected modulus and E_m is the modulus derived from the compression curves. Similarly, the collapse strength is corrected for density as:

$$\sigma = \sigma_m \left(0.1 / \rho \right)^{2.1} \tag{4}$$

where σ is the reported collapse strength and σ_m is that measured for each specimen.

The results of the compression tests are given in Figures 13a and 13b which show the average modulus and collapse strength for three replicate specimens over the entire

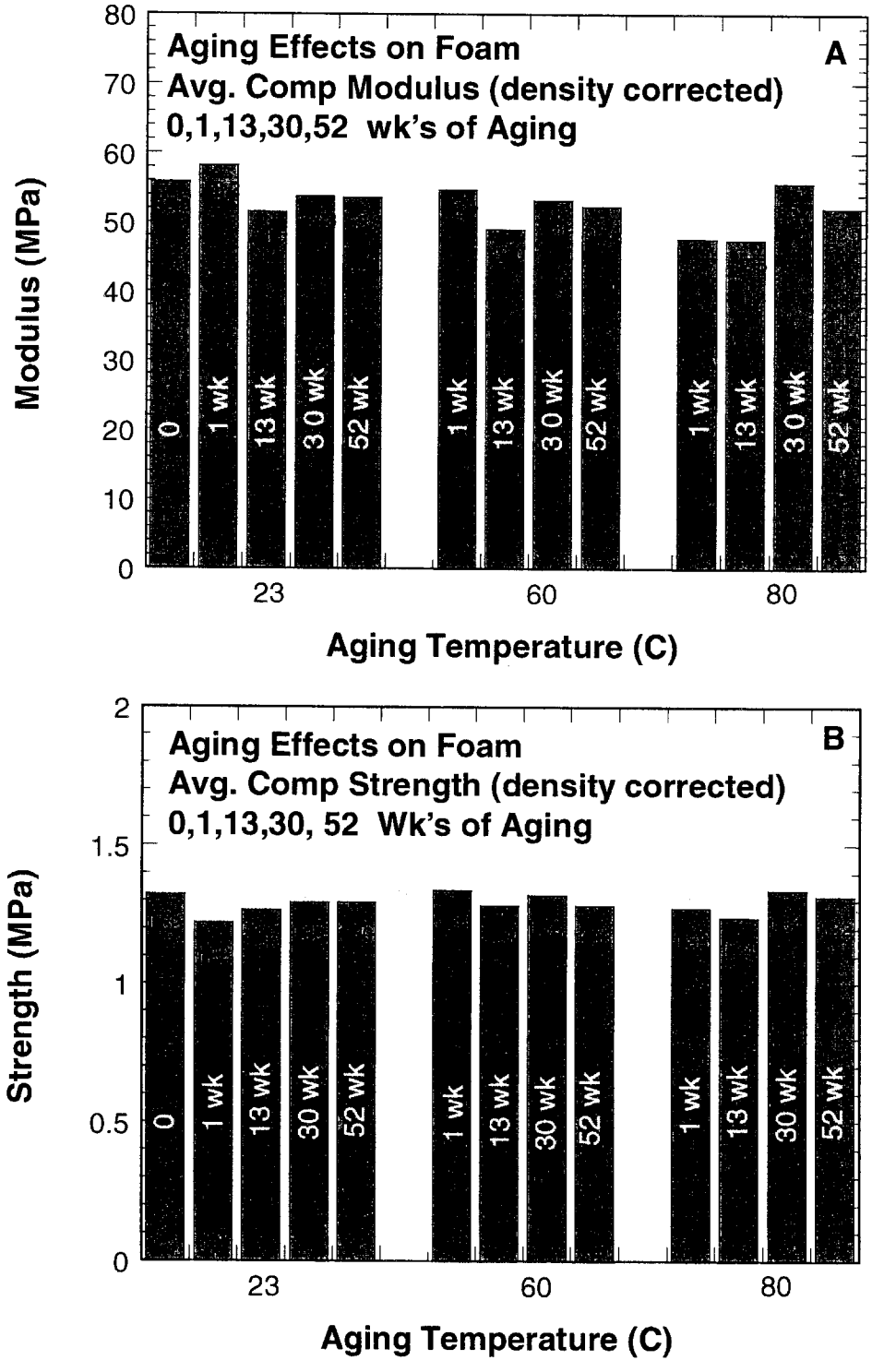

Figure 13. Summary of quasi-static compression testing. (a) The data do not reveal a clear aging effect with respect to a) modulus or (b) collapse strength after one year of aging.

aging matrix to date. The data do not reveal a clear aging effect with respect to modulus at present. Longer term testing is necessary to unambiguously determine the presence or absence of changes due to thermal aging. Collapse strength is less problematic. There appears to be little change due to aging.

tension behavior-

Figures 14a, b and c summarize the results for the aged specimens tested in tension. Only three aging intervals were examined: 1 week, 7 months and 1year. Baseline behavior is taken to be the average results for the specimens aged for 1 week at room temperature. No discernable trends are apparent with respect to either modulus, fracture strength or fracture strain for these tests. As with the quasi-static compression tests, longer aging periods may reveal time or temperature dependent changes in tensile properties.

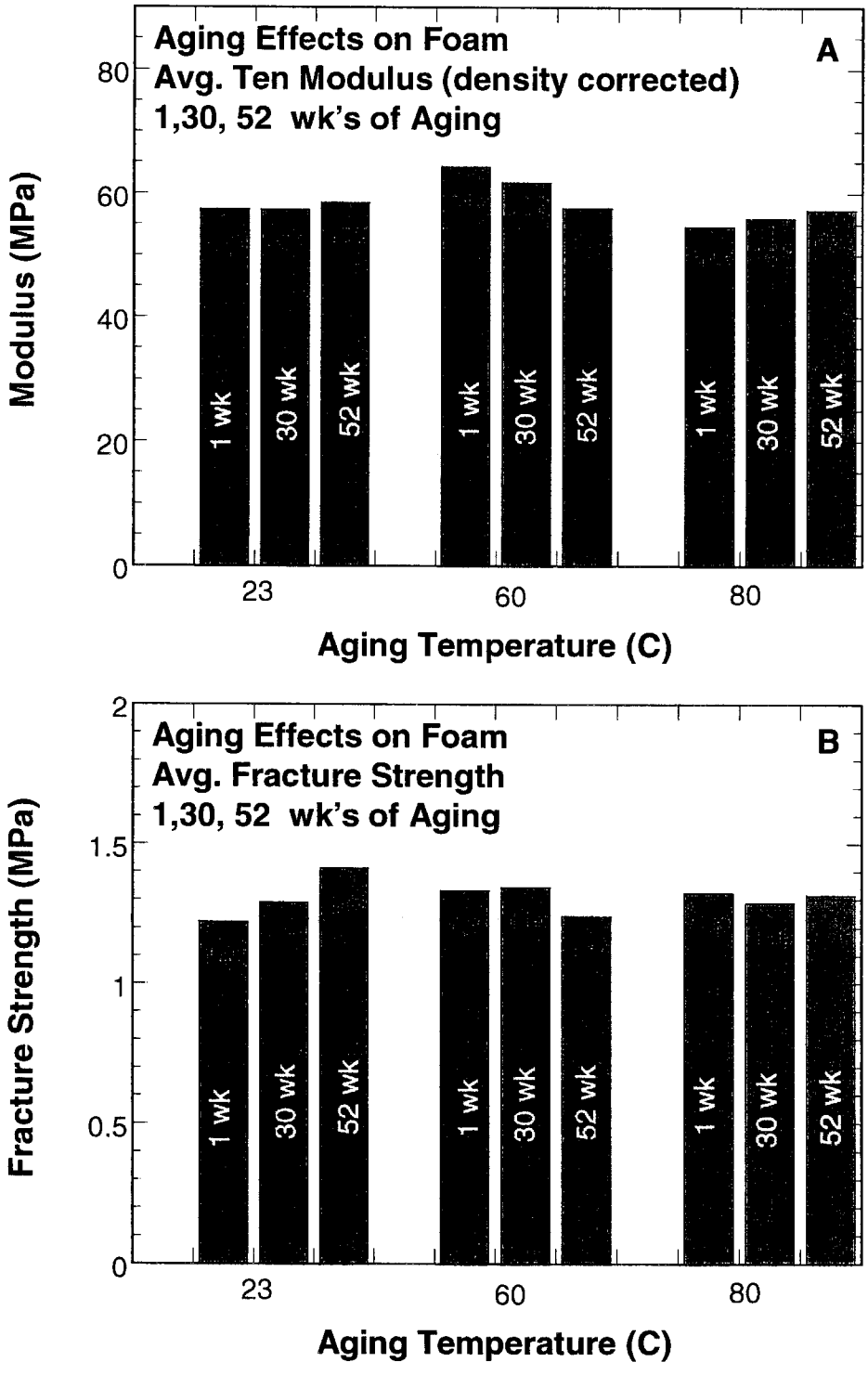

Figure 14. No systematic aging effects are evident with respect to tensile (a) modulus or (b) fracture strength.

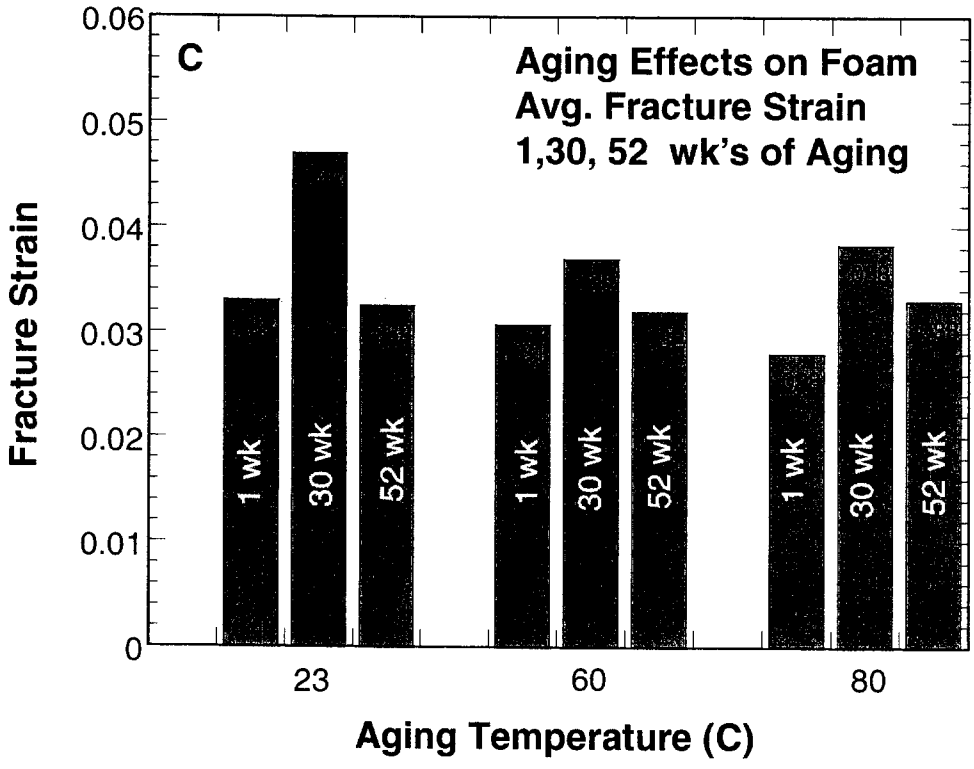

Figure 14. c) No systematic aging effects are evident with respect to tensile fracture strain.

IV. Conclusions

A systematic examination of thermal aging effects in a stockpile polyurethane foam has revealed changes in its impact properties, but not in more conventional quasi-static mechanical properties.

For the impact tests, two parameters were tracked as indicators of thermal aging effects, energy absorption (or toughness) and crush strength. Compared to the baseline energy absorption values, specimens aged to the longest time intervals, experienced a 12% (at 60°C) and 22% (at 80°C) loss in toughness. In contrast, crush strength of the aged foam under impact conditions was only minimally reduced, even at the longest time interval and at the highest temperatures. The loss in toughness resulted from the increased tendency of the aged foam to fracture or spall upon impact.

Unlike the impact specimens, there was no tendency for the specimens tested under quasi-static compression to fracture or spall with increasing aging temperature and time. The compression data did not reveal a clear aging effect with respect to modulus or collapse stress. Longer term testing is required to unambiguously determine the presence or absence of changes due to thermal aging. With regard to tensile behavior, no discernable trends are apparent with respect to either modulus, fracture strength or fracture strain. As with the quasi-static compression tests, longer aging periods may reveal time or temperature dependent changes in tensile properties.

Future efforts

Specimens will be prepared from aging blocks of foam and tested at the multi-year intervals to see if the trends with respect to impact testing continue and to see if additional aging yields effects with respect to the quasi-static tension and compression testing. DMA tests are planned to directly correlate the results presented here with any changes in dynamic properties that might be observed in aged foam. Additional studies will include examination of chemical changes of the polymer to account for the observations presented here.

Impact testing on free standing cylindrical specimens appears to be a sensitive tool for identifying the onset of aging induced changes in the mechanical properties of foams. Such tests should be considered in future programs where aging phenomena in foams are examined.

V. References

1. T. Ulibarri, *private communication*, Sandia National Laboratories, NM,
2. S.H. Goods, L.L. Whinnery, L. Sapochak and J. O'Toole, *unpublished research*
3. L.J. Gibson and M. F. Ashby, *Cellular Solids, Structure and Properties*, 2nd Edition, Cambridge University Press, Cambridge, UK, 1997
4. S.H. Goods, C.L. Neuschwanger, C. Henderson and D.Skala, *Mechanical Properties and Energy Absorption Characteristics of a Polyurethane Foam*, SAND97-8490, (March 1997)
5. S.H. Goods, C.L. Neuschwanger, L.L. Whinnery and W. D. Nix, *Mechanical Properties of a Particle-Strengthened Polyurethane Foam*, J. Appl. Polymer Sci., Vol. 74, p.2724, (1999)

DISTRIBUTION:

1 Honeywell FM&T
Attn: T. Wilson
R. Osborn
D. Speaker
2000 East 95th Street
PO Box 419159
D/830 SC-4
Kansas City, Missouri 64141

1 University of Nevada, Las Vegas
Department of Chemistry
Attn: Professor Linda Sapocak
Professor Allen L. Johnson
Box 454003
4505 Maryland Parkway
Las Vegas, NV 89154-4003

1 University of Nevada, Las Vegas
Department of Mechanical Engineering
Attn: Professor Brendan O'Toole
Box 454003
4505 Maryland Parkway
Las Vegas, NV 89154-4003

1 Los Alamos National Laboratory
Attn: J. Coons, MS C930
Weapon Materials & Manufacturing
Los Alamos, New Mexico 87545

1 L-092 G. B. Balazs

1 MS0311 G. E. Groves, 2616
1 MS0311 R. P. Roberts, 2616
3 MS0367 R. J. Salzbrenner, 1835
1 MS0447 P. D. Hoover, 2111
1 MS0834 A. M. Kraynik, 9114
1 MS0872 J. A. Sayre, 14001
1 MS0958 C. L. Adkins, 14172
1 MS0958 H. W. Arris, 14172
1 MS0958 E. A. Correa, 14172
1 MS0958 M. W. Donnelly, 14172
1 MS0958 J. A. Emerson, 14172
1 MS0958 M. J. Morrow, 14172
1 MS0958 R. L. Myers, 14172
1 MS0958 D. L. Zamora, 14172
1 MS1393 A. J. West, 2200

1	MS 1407	J. H. Aubert, 1811
1	MS 1407	R. L. Clough, 1811
1	MS 1407	R. R. Lagasse, 1811
1	MS 1407	E. M. Russick, 1811
1	MS 1407	D. R. Wheeler, 1811
1	MS9001	M. E. John, 8000
	Attn:	R. C. Wayne, 2200, MS9005
		J. Vitko, 8100, MS9004
		W. J. McLean, 8300, MS9054
		D. R. Henson, 8400, MS9007
		P. N. Smith, 8001, MS9002
		K. E. Washington, 8900, MS9003
		D. L. Crawford, 9900, MS9003
1	MS9013	W. R. Delameter, 2266
1	MS9013	R. D. Sauls, 2266
1	MS9034	R. Monson, 2263
1	MS9034	R. Van Cleave, 2263
1	MS9042	W. A. Kawahara, 8725
1	MS9042	W. Y. Lu, 8725
1	MS9108	C. W. Pretzel, 8414
1	MS9402	L. A. Domeier, 8722
1	MS9402	D. J. Irvin, 8722
1	MS9402	W. R Even, 8722
1	MS9402	P. N. Keifer, 8722
1	MS9402	D. M. Skala, 8722
1	MS9402	K. L. Wilson, 8722
10	MS9402	L. L. Whinnery, 8722
1	MS9402	B. C. Odegard, 8724
1	MS9403	J. C. F. Wang, 8722
10	MS9404	S. H. Goods, 8725
1	MS9404	J. R. Spingarn 8725
1	MS9405	T. M. Dyer, 8700
	Attn:	J. M. Hruby, 8702, MS9401
		D. E. Koker, 8709, MS9017
		R. Q. Hwang, 8721, MS9161
		E-P Chen, 8725, MS9042
		G. J. Thomas, 8724, MS9402
		J. L. Handrock, 8727, MS9042
		W. Perra, 8728, MS9042
		C. Henderson, 8729, MS9401
3	MS 9018	Central Technical Files, 8940-2
1	MS 0899	Technical Library, 4916
1	MS 9021	Technical Communications Department, 8528/ Technical Library, MS 0899, 4916
1	MS 9021	Technical Communications Department, 8528 For DOE/OST